arXiv:1404.6593v1 [astro-ph.IM] 26 Apr 2014

The Analytical Solution to the Temporal Broadening of a Gaussian-Shaped Radio Pulse by Multipath Scattering from a Thin Screen in the Interstellar Medium

M. M. McKinnon

National Radio Astronomy Observatory, Charlottesville, VA 22903 USA

ABSTRACT

The radio pulse from a pulsar can be temporally broadened by multipath scattering in the interstellar medium and by instrumental effects within the radio telescope. The observed pulse shape is a convolution of the intrinsic one with the impulse responses of the scattering medium and instrumentation. Until recently, common methods used to model the observed shape make assumptions regarding the intrinsic pulse shape and impulse responses, compute the convolution numerically, and solve for the pulse width and scattering timescale iteratively. An analytical solution is shown to exist for the specific case of the temporal broadening of a Gaussian-shaped pulse by a thin scattering screen. The solution is applied to multi-frequency observations of PSR B1834–10 to characterize the frequency dependence of its intrinsic pulse width and scattering timescale.

Subject headings: ISM – Stars – Data Analysis and Techniques – Astronomical Instrumentation

1. INTRODUCTION

The radio pulse from a pulsar can be temporally broadened by multipath scattering in the interstellar medium (ISM). The scattered light rays traverse a longer path than the rays propagating directly between the pulsar and the observer, and the concomitant time delay forms a scattering tail on the observed pulse. When the pulsed intensity is averaged over many rotations of the star, the observed pulse shape is the convolution of the intrinsic pulse shape with the impulse response of the scattering medium (Lee & Jokipii 1975). The analytical form of the impulse response is determined by the distribution of scattering material between the pulsar and the observer (Williamson 1972, 1973). If the scattering material is concentrated in a region that is thin in comparison to the distance between the pulsar and the observer and the plasma inhomogeneities in it follow a Gaussian power spectrum,

the impulse response is a truncated exponential characterized by a scattering timescale, τ_s (Cronyn 1970; Lee & Jokipii 1975). Many pulse shapes observed to have a scattering component are consistent with this "thin screen" approximation (Komesaroff et al. 1972; Löhmer et al. 2001, 2004; Bhat et al. 2004).

Free electrons in the ISM cause the broad-band radio pulse to be dispersed in time, with high frequency pulses arriving earlier than low frequency ones. The frequency dependence of the pulse arrival times follows a cold plasma dispersion law. The magnitude of the effect is characterized by the dispersion measure (DM), which is the electron density integrated along the line of sight to the pulsar. Since DM can be accurately measured, and only varies slowly with time if at all, its effects can be removed for the most part in constructing pulsar average profiles. Pulsar DMs and scattering timescales, which vary with both DM and frequency (e.g. Bhat et al. 2004), tend to be larger for those pulsars within the Galactic Plane and at large distances. DM measurements and independent estimates of pulsar distances can be used to construct models of the distribution of free electrons in the Galaxy (Taylor & Cordes 1993; Cordes & Lazio 2002). The models can be extended to include interstellar scattering using the scattering timescales extracted from pulsar average profiles (e.g. Cordes, Weisberg, & Boriakoff 1985; Bhat et al. 2004).

Pulse profiles computed from multi-frequency observations can be used to study the frequency dependence of τ_s and the intrinsic width of the pulsar's pulse. From a theoretical perspective, the scattering timescale should follow a power law, $\tau_s \propto \nu^{-\alpha}$, where the frequency scaling index is $\alpha = 4$ if the plasma inhomogeneities in the scattering medium follow a Gaussian power spectrum and $\alpha = 4.4$ for a Kolmogorov spectrum (Lee & Jokipii 1975; Rickett 1977). Multi-frequency observations of pulsars indicate the measured values of α are generally consistent with the theoretical ones (Komesaroff et al. 1972), although smaller scaling indices have been reported for highly dispersed pulsars (Löhmer et al. 2004; Bhat et al. 2004), suggesting a more uniform distribution of the scattering material and that the plasma inhomogeneties are non-Gaussian, perhaps following Lévy-Cauchy statistics (Boldyrev & Gwinn 2005). The frequency dependence of the intrinsic pulse width is also modeled as a power law with a scaling index in the range of 0.14 to 0.45, depending upon the model assumptions (Thorsett 1991 and references therein). The model of Ruderman & Sutherland (1975), for example, assumes the magnetic field in the emission region is dipolar in shape, the radiation is emitted at the local plasma frequency that varies with height in the magnetosphere, and the angular extent of the radiation is determined by the last field line to close within the star's corotating magnetosphere. These assumptions have led to the popular concept of a radius-to-frequency mapping (Cordes 1978) with the pulse width varying with frequency as $\nu^{-1/3}$. In general, pulse profiles are observed to widen with decreasing frequency. Observed values of the width's frequency scaling index, however, lie in the range

of about 0 to 1, and the width can tend towards a constant value at high frequency (Rankin 1983; Thorsett 1991). Owing to the different scaling indices in the frequency dependencies of the intrinsic width and scattering timescale, the observed pulse shape is heavily influenced by multipath scattering at low radio frequencies ($\nu \sim 100$ MHz), while it is essentially a replica of the intrinsic shape at high frequencies ($\nu \sim 10$ GHz). At moderate frequencies ($\nu \sim 1$ GHz), the pulsar's scattering timescale and intrinsic width can have comparable weight in shaping the observed pulse waveform.

Instrument related effects can also broaden the radio pulse in time. Wide bandwidth observations of pulsars are separated into narrow frequency channels to compensate for the effects of interstellar dispersion. The dispersion smearing of the pulse over this narrow detection bandwidth leads to a dispersion impulse response $d(t)$ characterized by a frequency-dependent timescale, τ_d. Additionally, detection circuitry in the radio telescope does not necessarily respond instantaneously to the pulse. It, too, has an impulse response, $i(t)$, with a time constant, τ_i. The observed pulse, $f(t)$, is then a convolution of the intrinsic pulse, $g(t)$, with the impulse responses of both the scattering medium, $s(t)$, and the instrument.

$$f(t) = i(t) * d(t) * s(t) * g(t) \tag{1}$$

A variety of methods have been developed to determine the intrinsic pulse width and the scattering timescale from the observed pulse profile by solving Equation 1. All have done so by computing the convolution numerically on an iterative basis and assuming functional forms for the instrumental impulse response functions. The first method adopts the thin screen approximation for $s(t)$, assumes the intrinsic pulse shape is a Gaussian, or sum of Gaussians, computes the convolution given by Equation 1 numerically, and solves for the pulse width and scattering timescale iteratively with a least squares fit of the observed profile to the computed profile (e.g. Ramachandran et al. 1997; Mitra & Ramachandran 2001; Löhmer et al. 2001, 2004). A second method uses Fourier inversion to deconvolve the intrinsic pulse shape from the impulse responses of the instrument and ISM. Since the Fourier transform of a convolution of functions is the product of their Fourier transforms (Bracewell 1986), one can compute the intrinsic pulse profile by assuming an $s(t)$, dividing the Fourier transform of the observed profile by the Fourier transform of $s(t)$, and Fourier transforming the result back to the time domain. Kuzmin & Izvekova (1993) demonstrated this method using different scattering functions. Bhat, Cordes, & Chatterjee (2003) developed a third method that makes no assumptions regarding the specific functional form of the intrinsic pulse shape and uses a CLEAN-based algorithm to determine the scattering timescale iteratively by requiring the deconvolved intrinsic profile to have "minimum asymmetry" and non-negative values of total intensity. The method also adopts the thin screen

approximation for $s(t)$. Bhat et al. (2004) extended this method to include a scattering function that corresponds to a uniformly distributed scattering medium with a square-law structure function. More recently, Demorest (2010) demonstrated a fourth method for determining the scattering function and intrinsic pulse profile that is based upon cyclic spectral analysis. Traditional spectral analysis procedures assume the pulsar signal is stationary over the timescale of the observation and only utilize the signal's amplitude. Demorest recognized that the pulsar signal is more accurately described as cyclo-stationary, allowing one to use the signal's amplitude and phase to determine $s(t)$ and $g(t)$ without any assumptions regarding their functional forms. Applying the method to PSR B1937+21, Demorest found the shapes of its pulse components to be Gaussian-like, while $s(t)$ was comprised of an exponential decay followed by a slowly decaying tail. As undeniably powerful as this method is, it can be computationally expensive, and recent work, such as that for fast radio bursts (Thornton et al. 2013), continues to use the more traditonal methods described above to estimate scattering timescales.

The purpose of this paper is to show that simple analytical solutions to Equation 1 exist in the specific case where the intrinsic pulse shape is Gaussian and $s(t)$ is the truncated exponential for a thin scattering screen. The solutions are derived in Section 2 using functional forms of $i(t)$ and $d(t)$ that are commonly found in the literature. In Section 3, the solution is applied to multi-frequency observations of PSR B1843–10 to illustrate the applicability of the solutions and to investigate the frequency dependence of the pulsar's width and scattering timescale.

2. TEMPORAL BROADENING ANALYSIS

The pulse broadening problem posed by the multiple convolutions in Equation 1 has an analytical solution when $g(t)$ is Gaussian, $s(t)$ is a truncated exponential, and $i(t)$ and $d(t)$ are any combination of Gaussians, truncated exponentials, and delta functions. The Gaussian pulse shape is

$$g(t,\mu) = \frac{S}{\sigma\sqrt{2\pi}} \exp\left[-\frac{1}{2}\left(\frac{t-\mu}{\sigma}\right)^2\right], \tag{2}$$

where S is the integrated flux density of the pulse, μ is its centroid, and σ is its standard deviation. The truncated exponential is

$$e(t,\tau) = \frac{1}{\tau}\exp(-t/\tau)H(t), \tag{3}$$

where τ is a time constant and $H(t)$ is the unit step, or Heaviside, function. $H(t)$ is equal to zero for $t < 0$, and one otherwise. Scattering conserves energy (Cronyn 1970), and the factor of $1/\tau$ in Equation 3 normalizes the impulse response so that the integrated flux density of the radio pulse is conserved in the convolution (Bhat, Cordes, & Chatterjee 2003).

2.1. Broadening Due to Scattering Only

In the absence of instrumental effects (i.e. $i(t) = d(t) = \delta(t)$), the pulse is broadened only by multipath scattering in the ISM, and the shape of the observed pulse is given by the convolution of Equations 2 and 3.

$$f(t,\tau) = \frac{S}{2\tau} \exp\left(\frac{\sigma^2}{2\tau^2}\right) \exp\left[-\frac{(t-\mu)}{\tau}\right] \left\{1 + \mathrm{erf}\left[\frac{t-(\mu+\sigma^2/\tau)}{\sigma\sqrt{2}}\right]\right\} \tag{4}$$

The function $w(x) = [1 + \mathrm{erf}(x)]/2$ within Equation 4 varies antisymmetrically from zero to one about $t = \mu+\sigma^2/\tau$, where its slope is maximum and varies inversely with σ. It attenuates the waveform for times much less than $t = \mu + \sigma^2/\tau$, and evolves into the step function, $H(t-\mu)$, as the pulse width becomes small with respect to the scattering timescale, $\sigma/\tau \ll 1$. In this case, $g(t)$ is a delta function in comparison to $s(t)$, and the convolution of $g(t)$ with $s(t)$ essentially replicates the exponential at $t = \mu$. Conversely, $f(t,\tau)$ is Gaussian-like in shape when $\sigma/\tau \gg 1$.

2.2. Broadening with Instrumental Effects Included

The instrumental impulse responses $i(t)$ and $d(t)$ in Equation 1 are assumed to have a variety of functional forms. For example, Ramachandran et al. (1997) and Mitra & Ramachandran (2001) consider the dispersion smearing and instrumental responses to be negligible. Thus, they assume the instrumental impulse responses are delta functions ($i(t) = d(t) = \delta(t)$), and Equation 4 is the analytical form of the numerical model they adopted. Similarly, Löhmer et al. (2001, 2004) suggest the rise times of the telescope receivers and back ends are small enough to consider the effect of $i(t)$ negligible ($i(t) = \delta(t)$). They model $d(t)$ as a rectangular function of width τ_d for incoherent dedispersion and $d(t) = \delta(t)$ for coherent dedispersion. Therefore, Equation 4 is the analytical form of their numerical model for their coherently dedispersed data.

Bhat, Chatterjee, & Cordes (2003) suggest the term $i(t) * d(t)$ is itself a convolution of many different truncated exponentials and effectively invoke the central limit theorem to

argue that its functional form is Gaussian. Since the convolution of two or more Gaussians is a Gaussian (e.g. Bracewell 1986), the broadening problem becomes the convolution of a single Gaussian with the truncated exponential from multipath scattering in the ISM. Equation 4 represents the analytical form of the numerical model adopted by Bhat, Chatterjee, & Cordes for the specific case when the intrinsic shape of their minimum asymmetry waveform is Gaussian, with μ in the equation replaced by the sum of the means of all Gaussian waveforms and σ replaced by the root sum square of their standard deviations. The equation also represents the solution to the pulse broadening problem when the instrumental impulse responses are both Gaussian in shape.

Cordes, Weisberg, & Boriakoff (1985) assume the instrumental impulse responses are truncated exponentials with different time constants. Post-detection signal integration in an analog filter bank can be accomplished with a simple electronic circuit consisting of a resistor and capacitor wired in series. The impulse response of the circuit is a truncated exponential with a post-detection time constant given by the product of the resistance and capacitance (e.g. Nayfeh & Brussel 1985; Fink & Christiansen 1982). When the impulse responses of the instrument and ISM are truncated exponentials, the observed waveform is

$$h(t) = e(t, \tau_i) * e(t, \tau_d) * e(t, \tau_s) * g(t) = E(t) * g(t), \tag{5}$$

where $e(t, \tau)$ is given by Equation 3, τ_s, τ_d and τ_i are the time constants for each impulse response, and $E(t)$ defines an impulse response for the entire system. Multiple convolutions of truncated exponentials form a linear combination of truncated exponentials (cf Williamson 1973), so that the system impulse response is

$$E(t) = \left[\frac{\tau_s \exp(-t/\tau_s)}{(\tau_s - \tau_d)(\tau_s - \tau_i)} - \frac{\tau_d \exp(-t/\tau_d)}{(\tau_s - \tau_d)(\tau_d - \tau_i)} + \frac{\tau_i \exp(-t/\tau_i)}{(\tau_s - \tau_i)(\tau_d - \tau_i)} \right] H(t). \tag{6}$$

The observed pulse, $h(t)$, is simply a linear combination of Equation 4 with different time constants.

$$h(t) = \frac{\tau_s^2 f(t, \tau_s)}{(\tau_s - \tau_i)(\tau_s - \tau_d)} - \frac{\tau_i^2 f(t, \tau_i)}{(\tau_s - \tau_i)(\tau_i - \tau_d)} + \frac{\tau_d^2 f(t, \tau_d)}{(\tau_s - \tau_d)(\tau_i - \tau_d)}. \tag{7}$$

Values of $h(t)$ calculated with Equation 7 are always non-negative, regardless of the time constant values. The equation is written under the assumption that $\tau_s > \tau_i > \tau_d$ so that the coefficients for each of the three $f(t, \tau)$ terms in it are non-negative. If the pulse width is also less than the scattering timescale but greater than the dispersion smearing and instrument response times, as is generally the case, the leading term in Equation 7 has the classic shape of an exponentially-broadened pulse, and the two trailing terms have narrow Gaussian shapes.

Equation 7 is the analytical form of the numerical model adopted by Cordes, Weisberg, & Boriakoff (1985) when the intrinsic pulse shape is Gaussian (see, for example, their Figure 1).

Examples of pulsar-intrinsic and scattered waveforms are shown in Figure 1. The Gaussian profile of the intrinsic pulse (Eqn. 2) is shown by the dotted line. The dashed line shows the intrinsic pulse scattered by a thin screen in the ISM (Eqn. 4), exclusive of any instrumental effects. The solid line shows the final observed pulse with instrumental effects included, assuming the instrumental impulse responses are truncated exponentials as included in Equation 7. The parameters used to compute the waveforms are listed in the figure caption. The integrated flux densities of the three waveforms are identical.

As written, the equations for the system impulse response (Eqn. 6) and the observed pulse (Eqn. 7) are indeterminate when any two, or all three, time constants are equal. When two of the time constants are equal, say $\tau_d = \tau_i$, the system impulse response and observed pulse are represented by

$$E(t) = \frac{\tau_s}{(\tau_s - \tau_d)^2}\left\{\exp\left(-\frac{t}{\tau_s}\right) - \exp\left(-\frac{t}{\tau_d}\right)\left[1 + \frac{t(\tau_s - \tau_d)}{\tau_s \tau_d}\right]\right\} H(t), \tag{8}$$

$$\begin{aligned} h(t) &= \left(\frac{\tau_s}{\tau_s - \tau_d}\right)^2 f(t, \tau_s) - \left[\frac{\tau_s \tau_d}{(\tau_s - \tau_d)^2} + \frac{t - (\mu + \sigma^2/\tau_d)}{(\tau_s - \tau_d)}\right] f(t, \tau_d) \\ &- \frac{\sigma^2}{\tau_d(\tau_s - \tau_d)} \exp\left(\frac{\sigma^2}{2\tau_d^2}\right) \exp\left[-\frac{(t-\mu)}{\tau_d}\right] g(t, \mu + \sigma^2/\tau_d), \end{aligned} \tag{9}$$

where $f(t, \tau_s)$, $f(t, \tau_d)$ are given by Equation 4 and $g(t, \mu + \sigma^2/\tau_d)$ is given by Equation 2. When all three time constants are equal to τ, the system impulse response and the observed pulse are

$$E(t) = \left(\frac{t}{\tau}\right)^2 \frac{e(t, \tau)}{2}, \tag{10}$$

$$\begin{aligned} h(t) &= \frac{[t - (\mu + \sigma^2/\tau)]^2 + \sigma^2}{2\tau^2} f(t, \tau) \\ &+ \left(\frac{\sigma}{\tau}\right)^2 \exp\left(\frac{\sigma^2}{2\tau^2}\right) \exp\left[-\frac{(t-\mu)}{\tau}\right] \frac{t - (\mu + \sigma^2/\tau)}{2\tau} g(t, \mu + \sigma^2/\tau). \end{aligned} \tag{11}$$

In another instrumental configuration where $i(t)$ is a delta function and $d(t)$ is a truncated exponential, the system impulse response and observed pulse are given by

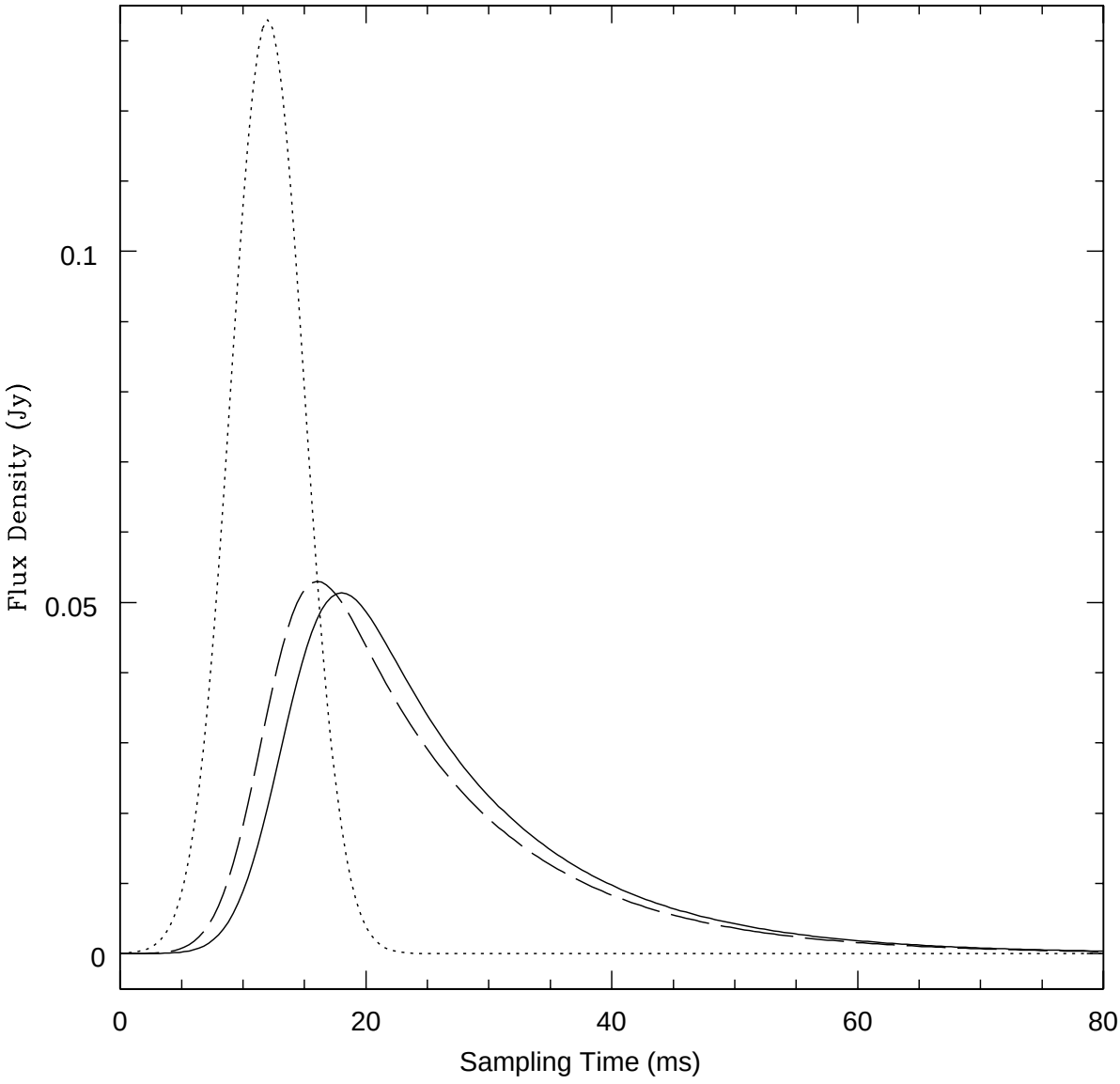

Fig. 1.— Temporal broadening of a Gaussian-shaped pulse. The pulsar-intrinsic Gaussian pulse (Eqn. 2) is shown by the dotted line. The intrinsic pulse broadened by scattering from a thin screen in the ISM (Eqn. 4), exclusive of any instrumental effects, is shown by the dashed line. The observed pulse with instrumental broadening terms included (Eqn. 7) is shown by the solid line. The parameters used to calculate the waveforms in the figure are $S = 1$ Jy, $\mu = 12$ ms, $\sigma = 3$ ms, $\tau_s = 12$ ms, $\tau_i = 1$ ms, and $\tau_d = 0.8$ ms.

$$E(t) = \frac{\exp(-t/\tau_s) - \exp(-t/\tau_d)}{\tau_s - \tau_d} H(t), \tag{12}$$

$$h(t) = \frac{\tau_s f(t, \tau_s) - \tau_d f(t, \tau_d)}{\tau_s - \tau_d}. \tag{13}$$

Equation 12 is also the mathematical representation of the two-component, thin screen scattering model discussed by Rankin & Counselman (1973), Isaacman & Rankin (1977), and Williamson (1973). Additionally, the equation may be interpreted as the representation of a pulse with the intrinsic shape of a truncated exponential that has been scattered by a single thin screen in the ISM. Equations 12 and 13 are also indeterminate when $\tau_s = \tau_d$. In this case, the system impulse response and observed pulse are given by

$$E(t) = \frac{t}{\tau} e(t, \tau), \tag{14}$$

$$h(t) = \frac{t - (\mu + \sigma^2/\tau)}{\tau} f(t, \tau) + \left(\frac{\sigma}{\tau}\right)^2 \exp\left(\frac{\sigma^2}{2\tau^2}\right) \exp\left[-\frac{(t-\mu)}{\tau}\right] g(t, \mu + \sigma^2/\tau). \tag{15}$$

3. APPLICATION

Multi-frequency observations of PSR B1834–10 were used to characterize the frequency dependence of the pulsar's scattering timescale and intrinsic pulse width by least squares fits of the data to relevant expressions derived in Section 2. The data were recorded by Gould & Lyne (1998) and are publicly available through the European Pulsar Network. The dispersion measure and topocentric rotation period of the pulsar at the time of the observation were 318.0 pc cm^{-3} and 563.707 ms, respectively. The instrumentation used to record the data consisted of a conventional analog filter bank followed by square law detectors. Therefore, Equation 7 is generally an appropriate model for the observation and was used in the fit to the data.

The parameters of the observations are described in Table 1. The table lists the observing frequency, the total bandwidth of the observation, the filter bandwidth, the number of samples (N) recorded across the pulsar's period, the sampling interval (t_s), and the dispersion smearing time over the filter bandwidth (τ_d). Gould & Lyne did not report the values of their post-detection integration times (τ_i), so τ_i was assumed to equal t_s in the fits. They also observed the pulsar at 408 MHz; however, that observation was not used in the analysis because its temporal resolution was too coarse ($N = 58$).

The results of the fits are listed in Table 2 and are illustrated in Figure 2. The pulse profiles at all four frequencies are simple, consisting of a single component, with the possible exception of an additional component of low intensity appearing on the trailing edge of the 925 MHz profile. The figure shows the model is a good representation of all four data sets, although the model slightly underestimates the 610 MHz profile in the region of the scattering tail. There is no evidence for temporal broadening due to interstellar scattering at 1642 MHz as that profile is consistent with a single component broadened only by instrumental effects. The large dispersion smearing caused by the large filter bandwidth used in the 1642 MHz observation causes the observed profile at that frequency to be wider than what one might expect from the profiles at 925 MHz and 1408 MHz.

A linear regression of the scattering timescales determined from the fits shows they follow a power law with a scattering timescale at 1 GHz of $\tau = 6.3^{+3.1}_{-2.1}$ ms and a frequency scaling index of $\alpha = 2.5^{+1.2}_{-1.1}$. Similar to results in Löhmer et al. (2001) and Bhat et al. (2004), the scaling index is smaller than the values of 4.0 or 4.4 expected from a Gaussian or Kolmogorov power spectrum for plasma inhomogeneities in the scattering medium. This result is also inconsistent with the assumption adopted in the derivation that the scattering is concentrated in a thin screen. The intrinsic widths, as represented by the values of σ determined from the fits, do not vary systematically with frequency, and are consistent within the errors with a constant value of $\sigma = 2.5$ over the observed frequency range.

4. SUMMARY

The temporal broadening of a Gaussian-shaped pulse by multipath scattering from a thin screen in the ISM was derived analytically for a variety of instrumental impulse response functions for the first time. The result was used to characterize the frequency dependence of the intrinsic pulse width and scattering timescale of PSR B1834–10. The intrinsic shape of the pulse is consistent with a single Gaussian component that varies little in width over a frequency range of 610 MHz to 1642 MHz. The frequency dependence of the pulsar's scattering timescale is flatter than what is expected from the canonical Gaussian and Kolmogorov power spectra for plasma inhomogeneities in the scattering medium.

The National Radio Astronomy Observatory is a facility of the National Science Foundation operated under cooperative agreement by Associated Universities, Inc. Part of this research has made use of the data base of published pulse profiles maintained by the European Pulsar Network, available at http://www.mpfir-bonn.mpg.de/pulsar/data/.

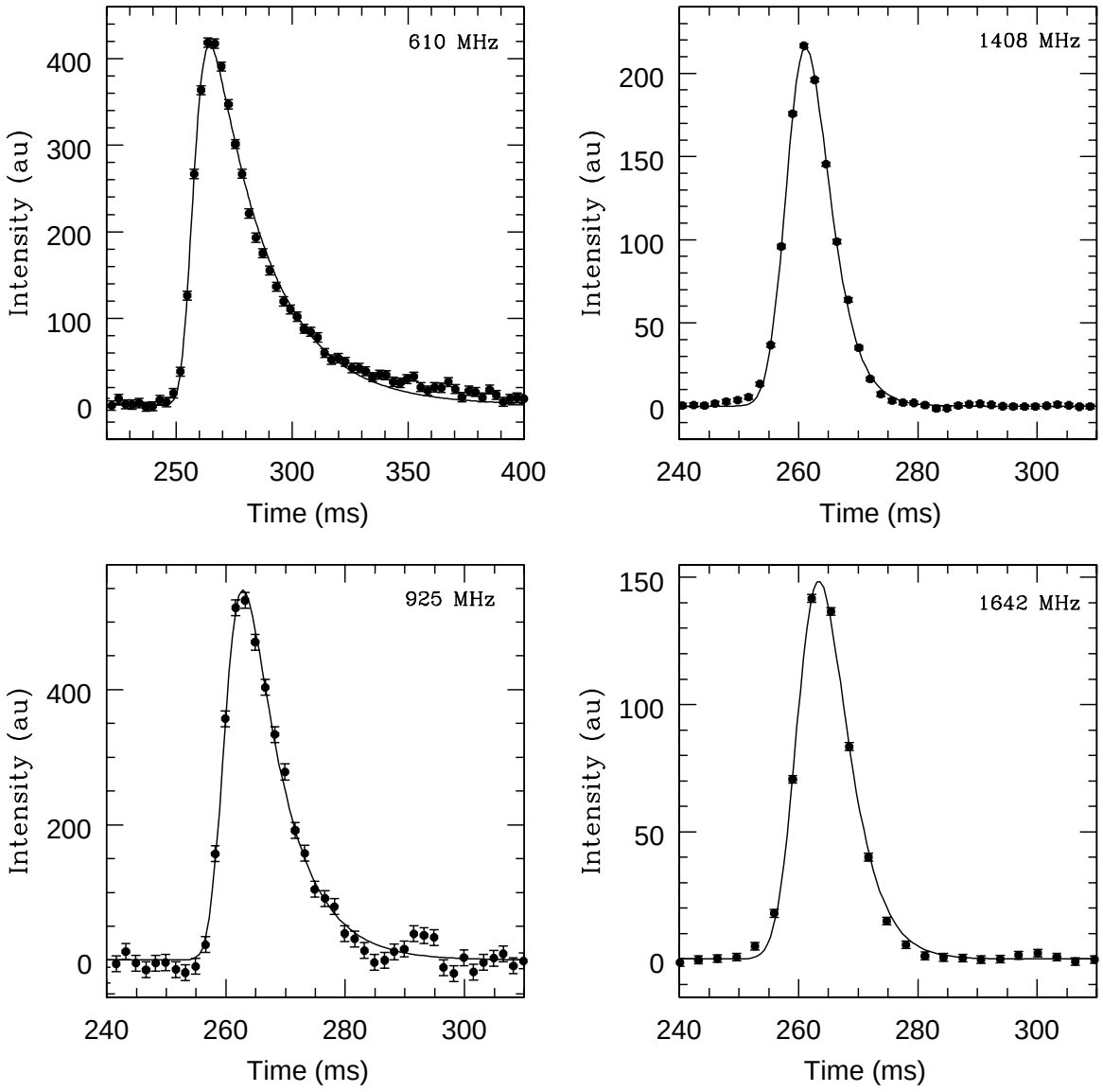

Fig. 2.— Temporal broadening of the pulse from PSR B1834–10 at four frequencies. The solid line in each panel of the figure is the best fit of Equation 7 to the data. The fit parameters are listed in Table 2. The scale of the error bars on the data points is equal to the off-pulse instrumental noise. The units of intensity are arbitrary (au).

REFERENCES

Bhat, N. D. R., Cordes, J. M., & Chatterjee, S., 2003, ApJ, 584, 782

Bhat, N. D. R., Cordes, J. M., Camilo, F., Nice, D. J., & Lorimer, D. R., 2004, ApJ, 605, 759

Boldyrev, S. & Gwinn, C. R., 2005, ApJ, 624, 213

Bracewell, R. N., 1986, The Fourier Transform and Its Applications, New York: McGraw-Hill, 230

Cordes, J. M., 1978, ApJ, 222, 1006

Cordes, J. M., Weisberg, J. M., & Boriakoff, V., 1985, ApJ, 288, 221

Cordes, J. M. & Lazio, T. J. W., 2002, astro-ph/0207156v3

Cronyn, W. M., 1970, Science, 168, 1453

Demorest, P. B., 2011, MNRAS, 416, 2821

Fink, D. G. & Christiansen, D., 1982, Electronics Engineers' Handbook, New York: McGraw-Hill, 16-2

Gould, D. M. & Lyne, A. G., 1998, MNRAS, 301, 235

Isaacman, R. & Rankin, J. M., 1977, ApJ, 214, 214

Komesaroff, M. M., Hamilton, P. A., & Ables, J. G., 1972, Aust. J. Phys., 25, 759

Kuzmin, A. D. & Izvekova, V. A., 1993, MNRAS, 260, 724

Lee, L. C. & Jokipii, J. R., 1975, ApJ, 201, 532.

Löhmer, O., Kramer, M., Mitra, D., Lorimer, D. R., & Lyne, A. G., 2001, ApJ, 562, L157

Löhmer, O., Mitra, D., Gupta, Y., Kramer, M., & Ahuja, A., 2004, A&A, 425, 569

Mitra, D. & Ramachandran, R., 2001, A&A, 370, 586

Nayfeh, M. H. & Brussel, M. K., 1985, Electricity and Magnetism, New York: Wiley, 397

Ramachandran, R., Mitra, D. Deshpande, A. A., McConnell, D. M., & Ables, J. G., 1997, MNRAS, 290, 260

Rankin, J. M., 1983, ApJ, 274, 359

Rankin, J. M. & Counselman, C. C., 1973, ApJ, 181, 875

Rickett, B. J., 1977, ARA&A, 15, 479

Ruderman, M. A. & Sutherland, P. G., 1975, ApJ, 196, 51

Taylor, J. H. & Cordes, J. M., 1993, ApJ, 411, 674

Thorsett, S. E., 1991, ApJ, 377, 263

Thornton, D. et al., 2013, Science, 341, 53

Williamson, I. P., 1972, MNRAS, 157, 55

Williamson, I. P., 1973, MNRAS, 163, 345

This preprint was prepared with the AAS LaTeX macros v5.2.

Table 1. Observational Parameters

Frequency (MHz)	Total BW (MHz)	Filter BW (MHz)	N	t_s (ms)	τ_d (ms)
610	4.0	0.125	189	3.0	1.5
925	8.0	0.250	337	1.7	0.8
1408	32.0	1.000	301	1.8	1.0
1642	40.0	5.000	177	3.2	3.0

Table 2. Results of Least Squares Fits

Frequency (MHz)	S (au)	μ (ms)	τ_s (ms)	σ (ms)	χ^2
610	5000 ± 260	250.7 ± 0.8	24.4 ± 2.0	3.2 ± 1.2	1.63
925	3910 ± 480	256.4 ± 0.7	6.4 ± 1.4	1.7 ± 1.1	1.11
1408	1110 ± 50	254.9 ± 0.2	2.9 ± 0.3	2.4 ± 0.3	1.62
1642	520 ± 30	255.9 ± 0.4	–	2.6 ± 0.4	1.13